PROCEEDINGS OF THE KECK GEOLOGY CONSORTIUM

Volume 35
2022-2023 Projects

Dr. Cameron Davidson and Dr. Karl Wirth, Editors
Co-Directors, Keck Geology Consortium

Theresa Klauer
Keck Geology Consortium Administrative Assistant
Macalester College

Keck Geology Consortium
Macalester College
1600 Grand Ave, St. Paul, MN 55105
(651) 696-6108, Info@KeckGeology.org

ISSN# 1528-7491
doi: 10.18277/AKRSG.2023.35

Funding Provided by:
Keck Geology Consortium Member Institutions
The National Science Foundation Grant NSF-REU 2050697

PROCEEDINGS OF THE KECK GEOLOGY CONSORTIUM

2022-2023 Projects

Cameron Davidson Editor and Co-Director Carleton College	Keck Geology Consortium Macalester College 1600 Grand Ave. St Paul, MN 55105	Karl Wirth Editor and Co-Director Macalester College

Keck Geology Consortium Member Institutions:

Amherst College, Beloit College, Carleton College, Colgate University, The College of Wooster, The Colorado College, Franklin & Marshall College, Macalester College, Oberlin College, Pomona College, Trinity University, Union College, Washington & Lee University, Wesleyan University, Whitman College

2022-2023 GATEWAY PROJECTS

EXPLORING LATE CRETACEOUS WETLAND ECOSYSTEMS PART 2: DINOSAURS AND VERTEBRATE MICROFOSSILS IN MONTANA
Faculty: KRISTI CURRY ROGERS and RAYMOND ROGERS, Macalester College
Peer Mentor: BROOKE NOONAN, Macalester College
Students: SOPHIA ESQUENET, Macalester College***;*** REBECCA FLOWERS, Carleton College***;*** BREANDA GOMEZ, Amherst College***;*** AUTUMN JESTER, Reynolds Community College
PEYTON LEWIS, Bowdoin College; MARISA LUFT, Macalester College; IRENE MÉNDEZ CURBELO, University of Puerto Rico Mayagüez; KATYA NICOLAYEVSKY, Colorado College

LANDSCAPE AND ENVIRONMENTAL CHANGE IN GLACIER NATIONAL PARK (GNP), MONTANA
Faculty: KELLY MACGREGOR, Macalester College and AMY MYRBO, Amiable Consulting
Peer Mentor: LOU MILLER, Macalester College
Students: JOSHUA BRUNS, Williams College; ALLISON HIDALGO, Washington and Lee University; EVELYN SOLIS CABRERA, Pitzer College; REYDALIZ TORRES LOPEZ, SUNY Geneseo

2022-2023 ADVANCED PROJECT

STRUCTURAL EVOLUTION OF A SEGMENTED NORMAL FAULT TRANSFER ZONE, SEVIER FAULT, SOUTHERN UTAH
Faculty: BEN SURPLESS, Trinity University
Students: AUDREY JENNINGS, Trinity University; JASPER NEATH, Trinity University; MICHELLE NISHIMOTO, Wellesley College

Conference Presentations – Montana Gateway Project

Mendez-Curbelo, I., Nicolayevsky, K., Luft, M., Flowers, R., Zugschwert, L., Curry Rogers, K., and Rogers, R.R., 2022, Tracking paleoenvironmental associations in vertebrate microfossil bonebeds in the upper Cretaceous (Campanian) Judith River Formation, Montana, Geological Society of America Abstracts with Programs, Vol 54, No. 5, doi:10.1130/abs/2022AM-379052.

Noonan, B., Lewis, P., Gomez, B., Esquenet, S., Jester, A., Rogers, L., Curry Rogers, K., and Rogers, R.R., 2022, Tiny modification features on fossil bones from vertebrate microfossil bonebeds in the upper Cretaceous (Campanian) Judith River Formation, Montana, Geological Society of America Abstracts with Programs, Vol 54, No. 5, doi:10.1130/abs/2022AM-379036.

Conference Presentations – Glacier Gateway Project

MacGregor, K., Bruns, J., Hidalgo, A., Miller, L., Solis Cabrera, E., Torres Lopez, R., and Myrbo, A., 2022, Sediment transport and deposition in Redrock and Fishercap lakes in Swiftcurrent Valley, Glacier National Park, Montana, USA, Geological Society of America Abstracts with Programs, Vol 54, No. 5, doi:10.1130/abs/2022AM-377951.

Miller, L., MacGregor, K., Van Wyk De Vries, M., Ito, E., Shapley, M.D., Brignone, G., and Romero, M., 2022, Using cesium-137 to determine sedimentation patterns in two proglacial lakes - Lago Argentino, Southern Patagonian Icefield, Argentina, and Lake Josephine, Glacier National Park, Montana, USA, Geological Society of America Abstracts with Programs, Vol 54, No. 5, doi:10.1130/abs/2022AM-377913.

Short Contributions – Utah Advanced Project

STRUCTURAL EVOLUTION OF THE SEGMENTED SEVIER NORMAL FAULT, SOUTHERN UTAH
BENJAMIN SURPLESS, Trinity University

MODELING FAULT-RELATED FRACTURING ASSOCIATED WITH A SEGMENTED NORMAL FAULT: IMPLICATIONS FOR GEOTHERMAL ENERGY POTENTIAL
AUDREY JENNINGS, Trinity University
Project Advisor: Benjamin Surpless

MODELING THE SEVIER FAULT ZONE, SOUTHERN UTAH: VALIDITY TESTING AND 3D ANALYSIS
JASPER NEATH, Trinity University
Project Advisor: Benjamin Surpless

NORMAL FAULT-TIP DAMAGE ZONE STRUCTURES AND GEOMETRIES FROM THE SEVIER FAULT, UTAH
MICHELLE NISHIMOTO, Wellesley College
Project Advisor: Katrin Monecke

KECK Geology Consortium
Learning Science Through Research
Published by the Keck Geology Consortium
Short Contributions
Keck Geology Consortium
Volume 35
May 2023
doi: 10.18277/AKRSG.2023.35.01

STRUCTURAL EVOLUTION OF THE SEGMENTED SEVIER NORMAL FAULT, SOUTHERN UTAH

BENJAMIN SURPLESS, Trinity University

INTRODUCTION

While it has long been recognized that major normal fault systems are commonly segmented in map view, as opposed to continuous, planar surfaces (e.g., Goguel, 1952; Tchalenko, 1970; Wallace, 1970; Schwartz and Coppersmith, 1984), only recently have researchers made significant advances in the role that segmentation plays in the evolution of these fault systems (e.g., Biddle and Christie-Blick, 1985; Crone and Haller, 1991; Peacock and Sanderson, 1996; Peacock, 2002). The geometry and relative strength of links between fault segments can strongly influence the propagation of slip during an earthquake (e.g., King and Nabalek, 1985; Crone and Haller, 1991; Zhang et al., 1991), and the perturbations of the local stress field caused by interaction of fault segments can influence the formation of relay ramps, minor faults, and associated fracture networks in transfer zones between synthetic normal fault segments (e.g., Peacock and Sanderson, 1996; Crider and Pollard, 1998; Faulds and Varga, 1998; Peacock, 2002).

In addition, the high fracture densities developed at these segment boundaries (e.g., Stock and Hodges, 1990; Hudson, 1992; Faulds, 1996) may enhance fluid flow, thus increasing rates of groundwater flow (e.g., Rowley, 1998), permitting hydrocarbon migration (e.g., Morley et al., 1990), or promoting ore mineralization (e.g., DeWitt et al., 1986). Because normal faults that typically develop in sedimentary basins, where natural resources commonly occur, are relatively planar and steeply-dipping in cross-section, with displacements of up to hundreds of meters (e.g., Peacock, 2002), well-exposed fault systems with these characteristics permit researchers to shed light on the evolution of similar faults in the subsurface. In this Keck Utah Advanced Project, students used the Sevier fault zone in southern Utah (Fig. 1), a segmented normal fault system with ~600 – 700 m dip-slip displacement, to investigate the structural evolution of a normal fault transfer zone across a range of spatial scales.

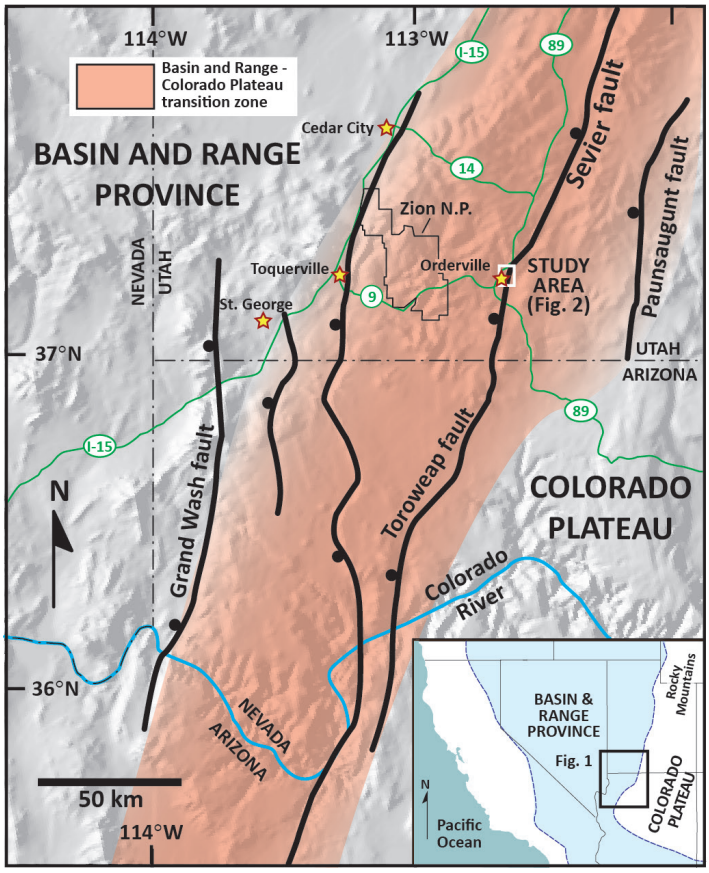

Figure 1. Physiographic context for the Sevier fault zone study area within the Basin and Range-Colorado Plateau transition zone (see inset). In combination with the Grand Wash, Hurricane, and Paunaugunt faults, the Sevier-Toroweap fault helps accommodate extension across the transition zone. Ball is on the hanging wall of the west-dipping faults. Detailed structure of the study area (boxed) is displayed in Figure 2. Digital shaded relief modified from Thelin and Pike (1991). Figure modified from Reber et al. (2001) and Surpless and McKeighan (2022).

STUDY AREA

The Sevier normal fault, considered one of the most important structures in the Basin and Range province (e.g., Davis, 1999; Lund et al., 2008), is part of the Toroweap-Sevier fault system, which extends for more than 300 km from northern Arizona to southern Utah (Fig. 1). The fault has accommodated extension across the transition zone from the Basin and Range province to the relatively stable Colorado Plateau since the Miocene (e.g., Reber et al., 2001; Lund et al., 2008), and previous workers have noted the potential of the fault to produce significant earthquakes (Anderson and Rowley, 1987; Doelling and Davis, 1989; Anderson and Christenson, 1989; Lund et al., 2008). It is likely that many segments of the Sevier fault reactivate older high-angle, Laramide-age contractional structures (e.g., Stewart and Taylor, 1996; Schiefelbein and Taylor, 2000), which may explain why the steeply-west-dipping fault zone is segmented in map view, with variations in the geometry of the linkages between normal fault segments (e.g., Davis, 1999; Reber et al., 2001; Schiefelbein, 2002; Doelling, 2008).

In this project, students focused their investigations on a particularly complex portion of the Sevier fault zone, termed the Orderville geometric bend (e.g., Reber et al., 2001) (Fig. 2). The Orderville bend displays a range of geometries associated with the interactions of three fault segments, which include the Mt. Carmel segment, the Orderville segment, and the Spencer Bench segment. The interaction of these 3 fault segments is likely responsible for the formation of the minor faults (displayed in white) and relay ramps shown adjacent to Red Hollow Canyon and Stewart Canyon (Fig. 2); these features likely evolved within the perturbed stress field associated with the transfer zones between dominant fault segments (Fig. 3).

STUDENT PROJECTS

The excellent vertical and lateral exposure of the Jurassic Navajo sandstone at the two primary study areas, at Red Hollow Canyon and Elkheart Cliffs (Fig. 2), provided students opportunity to directly observe faults, fractures, and deformation bands within these well-studied lithologies (e.g., Rogers et al., 2004; Schultz et al., 2010; Solom et al., 2010). The Elkheart Cliffs exposure (Fig. 2) displays the simplest fault geometry because the Mt. Carmel segment accommodates all E-W extension. In contrast, at Red Hollow Canyon, extensional strain is accommodated by a more complex system that includes the Orderville relay ramp and several other faults (Fig. 2). This spatial variation in fault complexity allows student researchers to treat these two locations as end members, permitting them to evaluate how the evolution of different fault geometries damages adjacent rock volumes (Fig. 3).

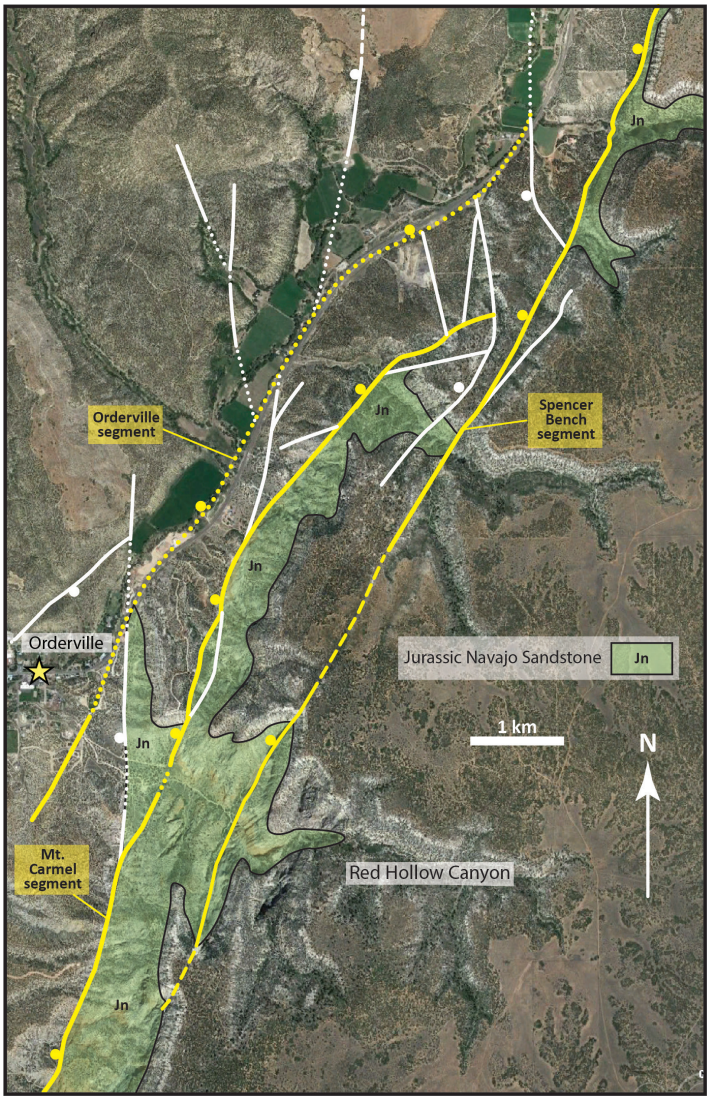

Figure 2. Structure map of the fault network within the Orderville geometric bend of the Sevier fault zone. Thick yellow lines are primary segments of the Sevier fault zone. Green shading indicates outcrop extent of the Jurassic Navajo Sandstone (Jn). Ball symbols on hanging wall of normal faults. Faults shown here are based primarily on mapping performed by Schiefelbein (2002) and our mapping, at 1:12,000 scale or larger. See Figure 1 for location. Figure modified from Surpless and McKeighan (2022).

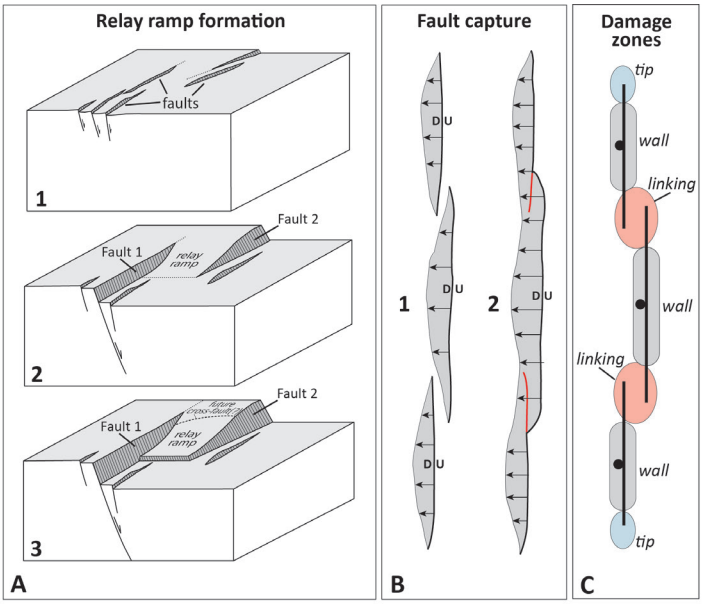

Figure 3. Diagrams displaying relay ramp development, fault capture, and damage zone classification. A) In all diagrams, the dark gray shaded area represents the magnitude of displacement, and the lines represent the slip direction as the hanging wall drops relative to the footwall. 1. A system of small-displacement faults develops to accommodate upper crustal stresses. The dotted lines represent the future propagation of the faults. 2. As displacement increases across the system, two faults (1 and 2) become dominant, both lengthening in map view and displaying increasing total displacement. A relay ramp forms in the zone of overlap between the faults. 3. Faults 1 and 2 link as a new cross-fault connects them. A future cross-fault may form where indicated, fully breaching the relay ramp. B) Map-view of a segmented fault system (bold lines are faults), with 1 and 2 representing progressive stages of fault segment linkage and capture. In 1, the three fault segments overlap but are only soft linked, and in 2, one of the segments has "captured" displacement from the other segments, isolating the overlapped portions of segments (red lines) that are no longer active. The segments are now hard linked and act as a single, corrugated fault. Arrows show the direction and relative magnitude of fault slip projected onto plan view. C) Schematic map view diagram of damage zone types associated with a segmented normal fault system (bold lines) with ball symbols on the hanging wall. Figure A. adapted from Peacock (2002) and Long and Imber (2011), Figure B. adapted from Reber et al. (2001), and Figure C. adapted from Kim et al. (2004).

To address fundamental questions about how rock volumes respond to the evolution of complex, segmented, normal fault systems, students applied a variety of approaches, including analysis of field data, 3D digital modeling and analysis of photographic data, development of a 3D retrodeformable model of the fault network based on previously published cross-sections and map data, and 3D stress-strain modeling of fault and fracture formation and propagation. Their work improves our understanding of the 3D evolution of fracture networks in complex normal fault zones, which has important implications for natural resource exploration.

Audrey Jennings (Trinity University) analyzed stress, strain, and fracture evolution using the Fault Response Modeling module of the Move 2020 software suite (by Petex). She created 3D models of a 2-fault-segment system, consistent with the approximate geometries of the Mt. Carmel and Spencer Bench segments of the steeply-dipping Sevier system (Fig. 2), at increasing levels of overlap. Models included a single layer defined by the mechanical properties of Navajo Sandstone, which is better exposed than any other lithology in the study area. Audrey modeled throw, stress, strain, and fracture orientation and intensity at varying fault slip displacements, ranging from 25 to 400 m.

All models showed the highest strain at fault tips, with strain also transferred between tips. Of her models, the less overlapped systems had the most intense strain fields between tips. Throw gradually changed from highly negative to slightly positive in this zone, indicating the initial development of a highly-fractured relay ramp, which thus would have high geothermal potential. In all models, fracturing is most intense in zones of elevated stress and strain fields, with fractures curving to connect tips, a feature best revealed in models where the fault segments display lesser overlap. Fracture intensity is higher in the hanging wall of segments, with vertical fractures roughly parallel to the fault. Due to predicted high strain and fracture density, Audrey confirmed that fault tips in segmented normal faults are promising for geothermal energy. Furthermore, she learned that slightly underlapped or overlapped faults represent the most likely setting for fracturing that might promote geothermal production.

Jasper Neath (Trinity University) used the Move2020 modeling suite (by Petex) to develop a viable 3D model of the complexly-segmented Sevier fault zone based on previously published geologic maps and cross-sections. He focused primarily on the fault network displayed in Fig. 2. With previously published geologic maps and cross-sections (Schiefelbein, 2002) as a base, he digitized geologic layers and fault horizons to build a 3D model of the fault network. He used his model to test the validity of initial cross-

sectional interpretations, because earlier subsurface interpretations in cross-sections were based on surface mapping rather than direct documentation of subsurface fault and layer geometries.

Because the cross-sectional lengths of individual layers should remain constant from their initial length to their deformed length, Jasper was able to test the viability of cross-section interpretations of subsurface structure with the restorable 3D models he developed. Where lengths were not consistent, we noted that subsurface model characteristics such as fault dip, magnitude of fault displacement, fault shape, spatial relationships between fault segments, or undocumented blind faults might be required. Jasper's work set the stage for future researchers, with the hope that eventually, several research questions can be addressed. These include: 1) How do the displacement and propagation of separate fault segments interact to form the present-day complexity exposed along the Orderville fault network? 2) How is strain accommodated along these fault zones at different stages of fault zone evolution? and 3) How do permeability and fluid flow pathways change as a segmented fault zone evolves?

Michelle Nishimoto (Wellesley College) used field data and Strucure-from-Motion (SfM) model analysis to investigate how fault-tip damage zones develop (Fig. 3) in response to fault propagation and displacement due to amplification of stresses at the fault tip. Because fractures initiate as a result of stresses exceeding rock strength and propagate based on the stress field at the fault tip, Michelle investigated the damage zone of the Spencer Bench segment near Orderville, Utah (Fig. 2), focusing on fractures that developed within the Jurassic Navajo Sandstone, the Temple Cap Formation, and the oldest beds of the Carmel Formation. Because normal faults grow laterally as slip and displacement increase, she focused on the tip zone of the Spencer Bench fault segment where fracturing is well-exposed.

Utilizing unmanned-aerial-vehicle (UAV) flights to capture high-resolution imagery of inaccessible rock exposures, Michelle constructed structure-from-motion (SfM) virtual outcrop models (VOMs) that she georeferenced and analyzed using Agisoft Metashape Professional, 3D modeling software. Based on those models, Michelle collected and analyzed fracture orientation and intensity data in the field and with VOMs.

Both types of data revealed an asymmetrical fracture intensity distribution proximal to the fault, with higher fracture intensity in the hanging wall relative to the footwall. The damage zone asymmetry she documented is consistent with some previous normal fault damage zones studies. Michelle also documented similar footwall damage zone widths in the same lithology, the Jurassic Navajo Sandstone, proximal to both the Mt. Carmel and Spencer Bench segments. Because the Mt. Carmel segment accommodates approximately 800 m dip-slip displacement while the Spencer Bench segment accommodates less than 10-m displacement, Michelle's work revealed that damage zone width must be established very early in the evolution of a fault, so damage zone width will not increase with increasing displacement.

ACKNOWLEDGEMENTS

This material is based upon work supported by the Keck Geology Consortium and the National Science Foundation under Grant No. 2050697. It was also supported by NSF Award 2042114 to PI Surpless. Finally, funding was provided by the Geosciences Department at Trinity University, including funding from the Roy and Tinker Funds to support undergraduate student research.

REFERENCES

Anderson, R.E., and Christenson, G.E., 1989, Quaternary faults, folds, and selected volcanic features in the Cedar City 1°x2° quadrangle, Utah: Utah Geological and Mineral Survey Miscellaneous Publication 89-6, 29 p.

Anderson, J.J., and Rowley, P.D., 1987, Geologic map of the Panguitch NW quadrangle, Iron and Garfield Counties, Utah: Utah Geological and Mineral Survey Map 103, 8 p. pamphlet, scale 1:24,000.

Biddle, K.T., and Christie-Blick, N., 1985, Strike – slip deformation, basin formation, and sedimentation, In: Biddle, K.T., Christie-Blick, N., Eds.: Strike– Slip Deformation, Basin

Formation, and Sedimentation. Society of Economic Mineralogists Special Publication, v. 37, p. 375– 386.

Crider, J., and Pollard, D., 1998, Fault linkage: Three-dimensional mechanical interaction between echelon normal faults: Journal of Geophysical Research, v. 103, p. 24,373 – 24,391.

Crone, A.J., and Haller, K.M., 1991, Segmentation and the coseismic behavior of Basin and Range normal faults: examples from east-central Idaho and southwest Montana, U.S.A.: Journal of Structural Geology, v. 13, p. 151– 164.

Davis, G., 1999, Structural geology of the Colorado Plateau region of southern Utah, with special emphasis on deformation bands: Geological Society of America Special Paper 342.

DeWitt, E., Thompson, J., and Smith, R., 1986, Geology and gold deposits of the Oatman district, northwestern Arizona: U.S. Geologic Survey Open-File Report 86-0638, 34 p.

Doelling, H.H., 2008, Geologic map of the Kanab 30'x60' quadrangle, Kane and Washington Counties, Utah, and Coconino and Mohave Counties, Arizona, 1:100,000-scale: Utah Geological Survey, MP-08-2DM.

Doelling, H.H., and Davis, F.D., 1989, The geology of Kane County, Utah, with sections on petroleum and carbon dioxide by Cynthia J. Brandt: Utah Geological and Mineral Survey Bulletin 124, 192 p., scale 1:100,000, 10 plates.

Faulds, J., 1996, Geologic map of the Fire Mountain 7.5' quadrangle, Clark County, Nevada, and Mohave County, Arizona: Nevada Bureau of Mines and Geology Map 106, scale 1:24,000 (with accompanying text).

Faulds, J., and Varga, R., 1998, The role of accommodation zones and transfer zones in the regional segmentation of extended terranes, In Faulds, J.E., and Stewart, J.H., Eds., Accommodation zones and transfer zones: the regional segmentation of the Basin and Range province: Geological Society of America Special Paper No. 343, p. 1 – 45.

Goguel, J., 1952, Traite de Tectonique: Masson, Paris (Translated by Thalmann, H.E., 1962). Tectonics: Freeman Publishing Company, San Francisco, 384 p.

Hudson, M., 1992, Paleomagnetic data bearing on the origin of arcuate structures in the French Peak – Massachusetts Mountain area of southern Nevada: Geological Society of America Bulletin, v. 104, p. 581 – 594.

Kim, K.-S., Peacock, D., and Sanderson, D., 2004, Fault damage zones: Journal of Structural Geology, v. 26, p. 503–517.

King, G.C.P., and Nabalek, J.L., 1985, The role of bends in faults in the initiation and termination of earthquake rupture: Science, v. 228, p. 984 – 987.

Long, J., and Imber, J., 2011, Geological controls on fault relay zone scaling: Journal of Structural Geology, v. 33, p. 1790 – 1800.

Lund, W.R., Knudsen, T.R., and Vice, G.S., 2008, Paleoseismic reconnaissance of the Sevier fault, Kane and Garfield Counties, Utah: Utah Geologic Survey Special Study 122, Paleoseismology of Utah, v. 16, 31 p.Lowe, D., 2004, Distinctive image features from scale invariant keypoints: International Journal of Computer Vision, v. 60, p. 91–110, doi: 10 .1023 /B: VISI .0000029664 .99615.94.

Morley, C., Nelson, R., Patton, T., and Munn, S., 1990, Transfer zones in the East African Rift system and their relevance to hydrocarbon exploration in rifts: American Association of Petroleum Geologists Bulletin, v. 74, p. 1234 – 1253.

Peacock, D.C.P., 2002, Propagation, interaction and linkage in normal fault systems: Earth-Science Reviews, v. 58, p. 121 – 142.

Peacock, D.C.P., and Sanderson, D.J., 1996, Effects of propagation rate on displacement variations along faults: Journal of Structural Geology, v. 18, p. 311 –320.

Reber, S., Taylor, W., Stewart, M., and Schiefelbein, I., 2001, Linkage and Reactivation along the northern Hurricane and Sevier faults, southwestern Utah, In XXX, Eds., The Geologic Transition, High Plateaus to Great Basin – A Symposium and Field Guide, The Mackin Volume: Utah Geological Association Publication 30, Pacific Section American Association of Petroleum Geologists Publication GB78, p. 379 – 400.

Rogers, C., Myers, D., and Engelder, T., 2004, Kinematic implications of joint zones and isolated joints in the Navajo Sandstone at

Zion National Park, Utah: Evidence for Cordilleran relaxation: Tectonics, v. 23, TC1007, doi:10.1029/2001TC001329.

Rowley, P., 1998, Cenozoic transverse zones and igneous belts in the Great Basin, Western United States: Their tectonic and economic implications In Faulds, J.E., and Stewart, J.H., Eds., Accommodation zones and transfer zones: the regional segmentation of the Basin and Range province: Geological Society of America Special Paper No. 343, p. 195-228.

Schiefelbein, I., 2002, Fault segmentation, fault linkage, and hazards along the Sevier fault, southwestern Utah [M.S. thesis]: Las Vegas, University of Nevada at Las Vegas, 132 p.

Schiefelbein, I., and Taylor, W., 2000, Fault development in the Utah transition zone and High Plateaus subprovince: Abstracts with Programs, v. 32, No. 7, p. 431.

Schultz, R., Okubo, C., and Fossen, H., 2010, Porosity and grain size controls on compaction band formation in Jurassic Navajo Sandstone: Geophysical Research Letters, v. 37, L22306, , doi:10.1029/2010GL044909.

Schwartz, D.P., and Coppersmith, K.J., 1984, Fault behavior and characteristic earthquakes – Examples from the Wasatch and San Andreas fault zones: Journal of Geophysical Research, v. 89, p. 5681 – 5698.

Solum, J., Brandenburg, J., Kostenko, O., Wilkins, S. and Schultz, R., 2010, Characterization of deformation bands associated with normal and reverse stress states in the Navajo Sandstone, Utah: AAPG Bull., v. 94, p. 1453–1475, doi:10.1306/01051009137.

Stewart, M., and Taylor, W., 1996, Structural analysis and fault segment boundary identification along the Hurricane fault in southwestern Utah: Journal of Structural Geology, v. 18, p. 1017 – 1029.

Stock, J., and Hodges, K., 1990, Miocene to recent structural development of an extensional accommodation zone, northeastern Baja California, Mexico: Journal of Structural Geology, v. 12, p. 312 – 328.

Surpless, B.E., and McKeighan, C., 2022, The role of dynamic fracture branching in the evolution of fracture networks: an outcrop study of the Jurassic Navajo Sandstone, southern Utah: Journal of Structural Geology, v. 161. DOI: 10.1016/j.jsg.2022.104664.

Tchalenko, J.S., 1970, Similarities between shear zones of different magnitudes: Bulletin of the Geological Society of America, v. 81, p. 1625–1640.

Thelin, G.P., and Pike, R.J., 1991, Landforms of the Conterminous United States - A Digital Shaded-Relief Portrayal: U.S.G.S. Geologic Investigations Series I – 2720.

Wallace, R.E., 1970, Earthquake recurrence intervals on the San Andreas fault: Bulletin of the Seismological Society of America, v. 81, p. 2875 – 2890.

Zhang, P., Slemmons, D.B., and Mao, F., 1991, Geometric pattern, rupture termination and fault segmentation of the Dixie Valley– Pleasant Valley active normal fault system, Nevada, U.S.A.: Journal of Structural Geology, v. 13, p. 165–176.

KECK Geology Consortium
Learning Science Through Research
Published by the Keck Geology Consortium
Short Contributions
Keck Geology Consortium
Volume 35
May 2023
doi: 10.18277/AKRSG.2023.35.02

MODELING FAULT-RELATED FRACTURING ASSOCIATED WITH A SEGMENTED NORMAL FAULT: IMPLICATIONS FOR GEOTHERMAL ENERGY POTENTIAL

AUDREY JENNINGS, Trinity University
Project Advisor: Benjamin Surpless

INTRODUCTION

Geothermal energy is a growing source of renewable energy in the United States, but it can be both technically challenging and financially risky to identify locations with high potential (e.g., Micale et. al., 2014). In order for a geothermal system to be conducive to any utility-scale electricity or heat generation, it must have high heat levels and pathways for fluid to flow. Faulting, which deforms rock and creates fluid pathways, can create an ideal scenario for geothermal energy production. By analyzing stress and strain distributions in certain fault zones, we may be able to locate productive systems. Faulds and Hinz (2015) describe high-density fracturing around segmented normal faults in extensional settings, making these zones promising for geothermal energy production. To explore the geothermal potential in segmented fault zones, I built 3D fault models in Move 2020 (by Petex) to assess displacement, stress, strain, and fracturing at different stages of fault interaction, which we compare to field data from the Sevier fault zone in southern Utah.

The Sevier fault zone is a NW-striking, segmented normal fault system that exhibits varying stages and types of fault segment interactions, including relay ramps and transfer zones that are associated with high-intensity fracturing (Surpless and McKeighan, 2022). Given the presence of these fracture-conducive geologic settings, we constructed 3D Move models based on the Sevier system in order to predict how vertical displacement, stress, strain, fracture orientation, and fracture intensity develop within a segmented, progressively overlapping normal fault system. With our work, we can investigate how fault segmentation and linkage affect stress and strain within a fault zone, and how stress and strain in these systems might evolve over time. We also can more definitively determine the effects of fault-related stress and strain on fracturing orientations and intensities within a given rock volume, as well as how stress, strain, and fracturing intensities and orientations evolve as fault segments propagate past each other. Finally, using both our modeling results and collected field data, we aim to develop new strategies for how to best utilize 3D modeling as a tool to efficiently identify locations with high geothermal potential, so that they can be targeted for further investigation.

BACKGROUND

At their most basic, geothermal systems require two primary factors: heat and flowing fluids. Heat flow has previously been well-mapped, indicating locations where geothermal energy may be possible (Boden, 2017). Geothermal systems tend to be productive at locations with average temperatures above 100 degrees C, but due to their subsurface location, identifying fluid flow pathways that will be conducive to geothermal systems can be much more difficult (e.g., Boden, 2017). Metrics to evaluate fluid flow potential include porosity and permeability. In general, highly permeable materials support geothermal systems, since connected open spaces allow for fluids to flow at high rates. However, permeability due to rock fracturing is especially important to identify when considering geothermal energy system viability, since fracture permeability can often be many orders of magnitude greater than matrix permeability. Given that researchers estimate that productive geothermal

systems must average a fluid flow rate of 200 kg/s, porosity simulation models predict that a fracture permeability of local material between 0.05 and 0.5 darcies is necessary to sustain a productive flow rate (1 darcy = volumetric flow rate of 1 cm^3/s of water with a viscosity of 1 centipoise over a cross-sectional area of 1 cm^2 under a pressure gradient of 1 atmosphere per centimeter) (e.g., Boden, 2017). Thus, identifying settings with high-level rock fracturing that produce permeability in these ranges will be key to establishing utility-scale geothermal energy production.

One promising location for geothermal energy is the Sevier fault zone in southern Utah. The Sevier fault has accommodated extensional strain between the Basin and Range Province and the Colorado Plateau since the Miocene (e.g., Surpless and McKeighan, 2022), and is a segmented normal fault that dips steeply to the west and exhibits 600 to 700 m of dip-slip displacement. Overlapping fault segments have led to complex structures, including relay ramps, fracture zones, and tip, wall, and linkage damage zones (e.g., Davis, 1999; Hecker, 1993; Smith and Arabasz, 1999). These types of structures are consistent with structural settings where geothermal systems form (e.g., Curewitz and Karson, 1997; Faulds and Hinz, 2015). Localities that exhibit combinations of these settings, which we have documented along the Sevier fault, suggest that the Sevier fault is a promising location for understanding how and where high-geothermal potential systems develop. Of the structural settings commonly linked to high geothermal potential, two that are especially common within segmented normal fault systems are the regions between interacting fault tips and across relay ramps. As fault tip stress zones approach one another, they may begin to interact and cause new deformation (Fig. 1). Such "transfer zones" can result in the development of relay ramps, structures that connect the hanging wall of one fault segment to the footwall of another segment and help facilitate the transfer of strain and slip between the two segments (Fig. 2).

Relay ramp formation depends on the specific geometry and relationship between involved fault segments; if segments are too far apart, they will not interact. If segments are more closely spaced, as

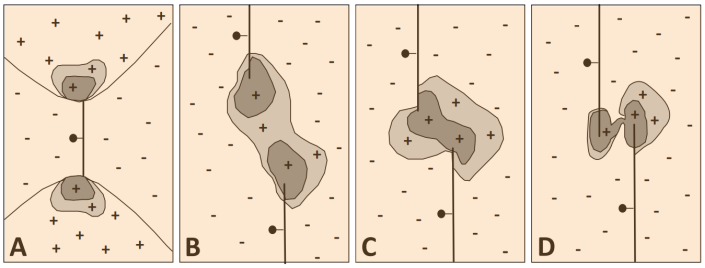

Figure 1. Map view of lateral fault segment propagation and associated stress field changes (elevated stress shown in gray and dark gray. - symbols correspond to areas where failure is not likely to occur as the fault continues to propagate. Diagram A modified from Cowie and Shipton (1998), and diagrams B - D modified from Crider and Pollard (1998) and Crider (2001).

segments propagate past each other, deformation in stress transfer zones and along relay ramps increase, and the relay ramp may become breached, physically linking the two fault segments into one system (Fig. 2) (e.g., Trudgill and Cartwright, 1994; Crider and Pollard, 1998). Importantly, spacing and geometry of faults affect whether fault linkage occurs and ultimately how fault linkage occurs. Fault dip and the subsurface distance between fault tip lines most strongly affect the likelihood of linkage (Crider and Pollard, 1998). Linkage of overlapping faults typically includes an interaction phase during which a relay ramp forms due to stress field interactions between faults (e.g., Crider, 2001; Crider and Pollard, 1998). Relay ramps connect the hanging wall of one fault segment to the footwall of another segment, effectively transferring strain and/or slip between the two segments, and may ultimately directly link the faults to form a single segmented fault (e.g., Larsen,

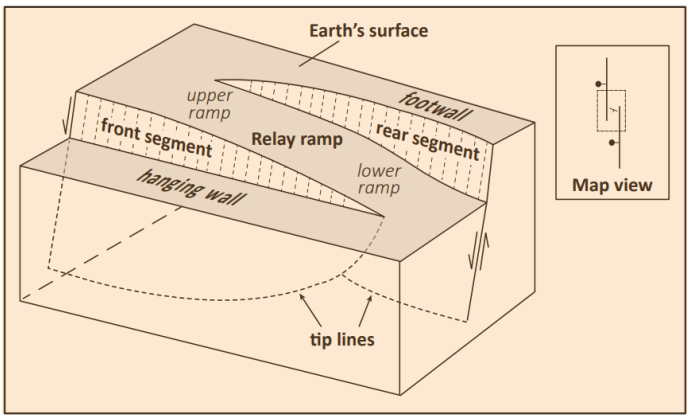

Figure 2. Diagram of a relay ramp developing between en echelon normal fault segments. Within the fault scarps, fault slip tapers to zero at the tips. The insert shows a map view of the relay ramp, with the fault segments represented by parallel lines and the dashed box indicating the location of the 3D diagram. Figure modified from Trudgill and Cartwright (1994) and Crider and Pollard (1998).

1988; Morley et al., 1990; Peacock and Sanderson, 1991; Trudgill and Cartwright, 1994; Crider and Pollard, 1998; Faulds and Varga, 1998; Walsh et al., 1999; Peacock et al., 2000; Ferrill and Morris, 2001; Reber et al., 2001; Camanni et al., 2019).

METHODS

The Fault Response Modeling (FRM) module of Petex's Move 2020 modeling software calculates variables including displacement, strain, and stress within a user-defined fault system using elastic dislocation theory calculations at "sampling" points within a user-defined medium (Petex, 2020). With the FRM module, we created a total of 16 fault models mimicking a segmented normal fault system, based on the geometry of the Sevier fault zone. A simplified description of the modeling process and the lithological conditions of the observation layer are presented in Fig. 3 and Table 1, respectively. The fault model consists of two parallel en echelon fault segments, each ten kilometers long, 1 kilometer apart, and dipping 70 degrees. This configuration approximates the observed geometry of interacting fault segments within the real Sevier fault zone. In order to mimic simultaneous vertical throw and horizontal displacement, we assigned progressive amounts of displacement (of 5, 25, 50, and 150 m) to four models that also experienced progressive lateral propagation. Thus, a model with two laterally separated fault segments (such that no interaction occurred between them) experienced 5 m of slip, a model with the fault segment tips placed even with one another experienced 25 m of slip, a model with 1 km of overlap between fault segments experienced 50 m of slip, and a model with 3 km of overlap between fault segments experienced 150 m of slip.

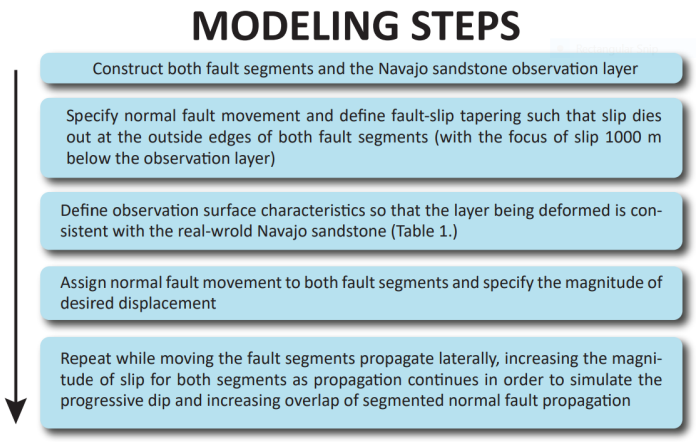

Figure 3 . Workflow for creating 3D models of the Sevier fault zone in the Fault Response Modeling module of MOVE 2020.

Table 1. Rock and fault properties used in this study.

NAVAJO SANDSTONE PROPERTIES	
POISSON'S RATIO	0.25
YOUNG'S MODULUS	30,000 MPa
COEFFICIENT OF FRICTION	0.40
FRICTION ANGLE	30 degrees
COHESION	2.00 MPa
DENSITY	2,459 kg/m³

FAULT PROPERTIES	
FREE SURFACE ELEVATION	0.0 m
DEPTH OF MAXIMUM SLIP	-1,000 m
DISPLACEMENT	Defined by slip
OPENING SLIP MAGNITUDE	0.0 m
DIP ANGLE	70 degrees

These slips occurred along an elliptical displacement gradient on the fault plane, with the greatest amount of slip equidistant from the fault tips and at 1 kilometer below the observation surface, and 0 slip at the fault tips. Such dimensions meant that the slip occurred across the "no interaction" model at a gradient of 1 m/km, across the "even" model at a gradient of 5 m/km, across the "1 km overlap" model at a gradient of 10m/km, and across the "3 km overlap" model at a gradient of 30 m/km from the foci to the fault tips. We generated 16 models showing vertical displacement, maximum coulomb shear stress, strain dilation, and predicted fracture intensity and orientation based on the 4 given fault configurations. Though our models do not precisely match the fault geometry of the Sevier or the complete stratigraphy, they do represent the general fault interactions within the system and therefore can be used to gain better insight into the distribution of fracturing and enhanced permeability within the Sevier fault zone. By comparing our modeled results to the fracture networks documented along the Sevier fault zone (Nishimoto, this volume), we can validate our modeling process and draw general conclusions about faulting and fracturing within segmented normal fault systems.

RESULTS

Our modeling results reveal how vertical displacement, stress, strain, fracture orientation, and fracture intensity vary across a range of total

displacements and fault geometries (Fig. 4). Model results are shown with a heatmap, with values increasing from the lowest (shown in blue), to the highest (shown in red). Fault geometry affects the distribution of throw, stress, strain, and fracturing across models with progressive displacement and relative overlap. The fault segments show two separate stress fields in the "no interaction" model, but the fields begin to converge with the "even" model and continue to do so as the segments become increasingly overlapped. Since the models mimic the Sevier fault zone, rather than perfectly replicating it, we cannot use the models to predict specific throw, stress, and strain values; however, we can use these values for general comparisons between models. Thus, it appears that stress and strain values increase as fault segment overlap progresses. In the greatly overlapped model (with 3 km of overlap and 150 m of slip), calculated maximum Coulomb shear stress values reach a maximum of 186.3 MPa along the fault plane; in the no-interaction model experiencing 5 m of slip, the maximum calculated maximum Coulomb shear stress value occurs along the fault plane as well, but only at 0.9 MPa. Strain dilation varies similarly, with the maximum strain dilation value recorded as 0.000 in the no-interaction model and 0.0011in the 3 km overlap model, occurring in all models near the fault tips and in the hanging wall (HW) of the system.

Even within individual models, throw, stress, strain and fracturing vary across parts of the fault system. For all of our models, stress and strain are largely concentrated at the fault tips, and overall stress is greatest in the footwall while strain is greatest in the hanging wall. Our models also show high-intensity fracturing concentrated at fault tips and in the hanging wall of fault systems. Fractures are generally oriented parallel to the fault segment(s) in the hanging wall, and more perpendicular to the fault in the footwall. At the tips, where strain is greatest and stress fields are

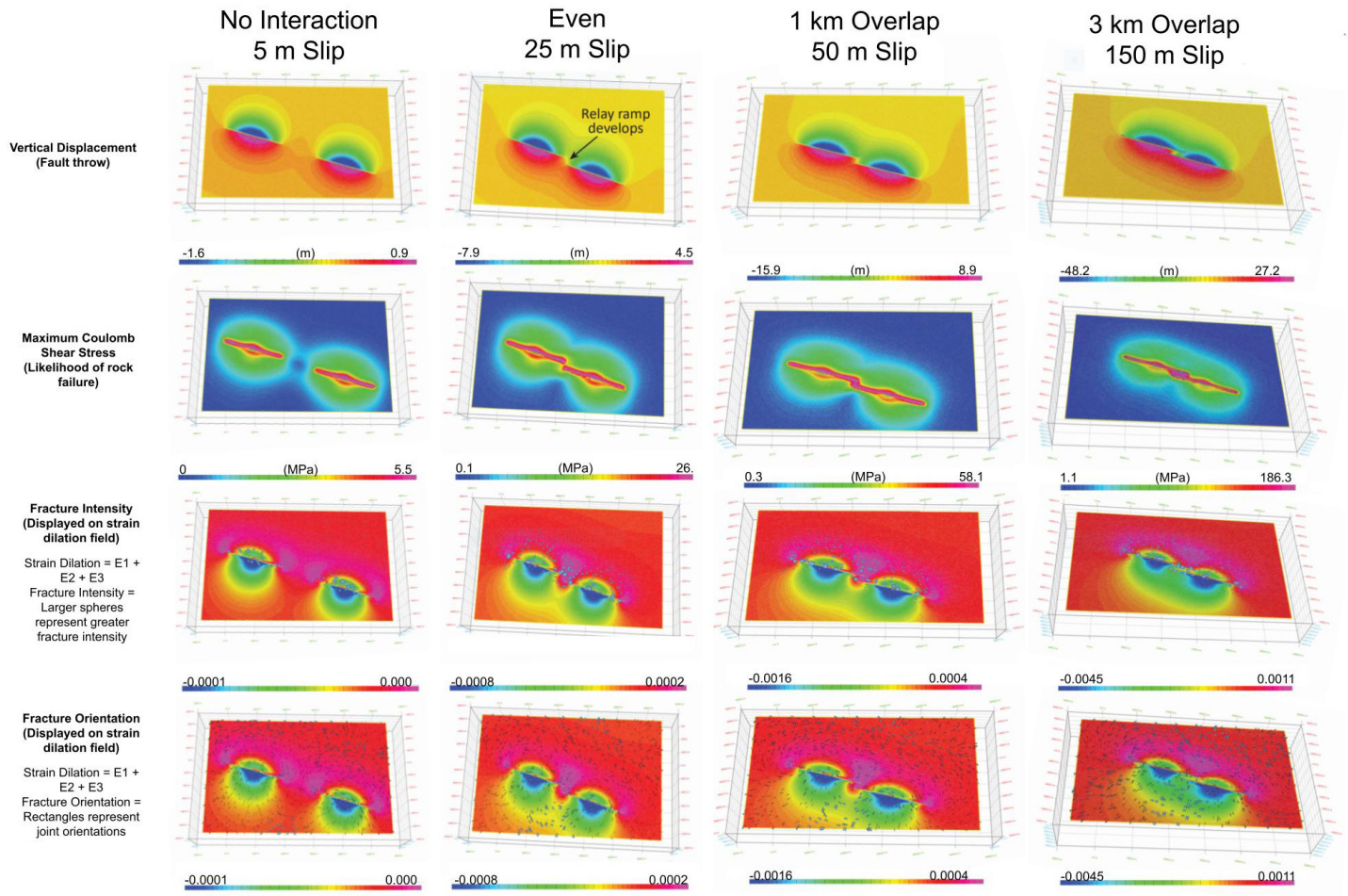

Figure 4. Modeling results, showing vertical displacement, maximum coulomb shear stress, strain dilation, fracture intensity, fracture orientation.

interacting between segments, the fracture orientations are much more variable than in the midsection of the fault system.

In addition, prior modeling of fault interactions reveal that the greatest Coulomb stress occurs along the relay zone between fault segments where tips of the different segments are closest (Crider and Pollard, 1998). Our results support these findings, with yellow lines on the models representing higher maximum stress and strain from the northernmost tip of the western segment to the northernmost tip of the eastern segment. Strain generates fractures in rock in alignment with our models which show high-intensity fracturing at fault tips where strain is concentrated. However, fault segments with extreme overlap experience less shear Coulomb stress relative to applied load when compared to underlapped fault segments (Crider and Pollard, 1998), so the increase in maximum stress within the relay zone in our overlapped model is relatively small.

DISCUSSION

Our results indicate that segmented normal fault systems with significant levels of overlap between fault segments present a promising location for further geothermal investigation due to the higher intensity fracturing present, relative to single or underlapped systems. Specifically, fracturing intensity appears especially elevated between overlapped fault tips (at mid-to-high levels of vertical displacement) as well as along relay ramp development zones between fault tips. These locations have also been identified as having especially high stress and strain in prior fault-linkage models with similar geometries (Crider and Pollard, 1998). Given the strong relationship between high levels of stress, strain, and elevated fracture intensity, our models seem to support Crider and Pollard's (1998) analysis of high-stress and strain areas in fault linkage systems and also indicate that such locations may be high in geothermal energy potential. From our models, it also appears that the hanging wall of segmented normal fault systems (with higher fracture intensities than the footwall) demonstrate more promise for fluid flow and thus geothermal energy. Targeting further geothermal research in such geological formations could be an important step in finding new ways to harness the Earth's heat, and further encourage both public and private investment in geothermal projects (e.g., Micale et. al., 2014). However, applying the proper geothermal energy system to the geological constraints of the specific fault zone will be critical to properly using any local potential.

Our models indicate that the intensities and orientations of subsurface fracturing that would be conducive to geothermal energy are likely present within the overlapped, normal Sevier fault zone, but the temperature levels within this specific fault system are likely too low or too inconsistent to provide usable geothermal electricity given current geothermal infrastructure (Boden, 2017). However, we can generalize the displacement, stress, strain, and fracturing patterns we see in our models to other segmented normal fault systems that are in geothermally warmer or more accessible regions, using our data to indicate where within such systems we may expect to see the greatest potential and what factors (like fault geometry or amount of slip) contribute most greatly to the development of geothermal potential. Ultimately, the relative agreement between our fracture modeling results and the damage zone data collected during fieldwork along the Sevier fault (Nishimoto, this volume) illustrates the potential for 3D modeling to help identify regions with high geothermal potential. Given that one main obstacle to expanding geothermal energy is the difficulty in identifying high-potential geothermal systems, improving modeling strategies for predicting the fracturing intensity and thus fluid flow potential of different geologic settings is an important step in making utility-scale geothermal energy a feasible future solution.

ACKNOWLEDGMENTS

This material is based upon work supported by the Keck Geology Consortium and the National Science Foundation under Grant No. 2050697. It was also supported by NSF Award 2042114 to PI Surpless. Finally, funding was provided by the Geosciences Department at Trinity University, including funding from the Roy and Tinker Funds to support undergraduate student research.

REFERENCES

Boden, D.R., 2017, Geologic Fundamentals of Geothermal Energy: Boca Raton, Florida, CRC Press, 399 p.

Cowie, P.A., and Shipton, Z.K., 1998, Fault Tip Displacement Gradients and Process Zone Dimensions, Journal of Structural Geology, v. 20, p. 983 - 997.

Crider, J., 2001, Oblique Slip and the Geometry of Normal-Fault Linkage: Mechanics and a Case Study from the Basin and Range in Oregon, Journal of Structural Geology, v. 23, 12, p. 1997 - 2009.

Crider, J., and Pollard, D., 1998, Fault linkage: Three-dimensional mechanical interaction between echelon normal faults, Journal of Geophysical Research, v. 103, p. 24.373 - 24.391.

Curewitz, D., and Karson, J. A., 1997, Structural settings of hydrothermal outflow: Fracture permeability maintained by fault propagation and interaction, J. Volcanol. Geotherm. Res., v. 79, p. 149 - 168.

Davis, G.H., 1999, Structural geology of the Colorado Plateau region of southern Utah: Geological Society of America Special Paper 342, p. 127.

Doelling, H.H., 2008, Geologic map of the Kanab 30'x60' quadrangle, Kane and Washington Counties, Utah, and Coconino and Mohave Counties, Arizona, 1:100,000-scale: Utah Geological Survey, MP-08-2DM

Faulds, J., and Hinz, N., 2015, Favorable Tectonic and Structural Settings of Geothermal Systems in the Great Basin Region, Western USA: Proxies for Discovering Blind Geothermal Systems, in Proceedings, World Geothermal Congress, Melbourne: Australia, Nevada Bureau of Mines and Geology (https://www.osti.gov/servlets/purl/1724082).

Hecker, S., 1993, Quaternary tectonics of Utah with emphasis on earthquake-hazard characterization: Utah Geological Survey Bulletin, v. 127, p. 1 - 31.

Micale, V., Oliver, P., and Messent, F., 2014, The Role of Public Finance in Deploying Geothermal: Background Paper, in San Giorgio Group Report, Climate Policy Initiative, p. 1 - 15.

Petex, 2020, Move 2020 Tutorial 33: Fault Response Modeling.

Schiefelbein, I., 2002, Fault segmentation, fault linkage, and hazards along the Sevier fault, southwestern Utah [M.S. thesis]: Las Vegas, University of Nevada at Las Vegas, 132 p.

Smith, R.B., and Arabasz, W.J., 1991, Seismicity of the Intermountain Seismic Belt, in Slemmons, D.B., Engdahl, E.R., Zoback, M.D., and Blackwell, D.D., eds., Neotectonics of North America: Geological Society of America, p. 185 - 228.

Schultz, R., 2010, Porosity and Grain Size Controls on Compaction Band Formation in Jurassic Navajo Sandstone: American Geological Union geophysical Research Letters v. 37, 22.

Surpless, B.E., and McKeighan, C., 2022, The role of dynamic fracture branching in the evolution of fracture networks: an outcrop study of the Jurassic Navajo Sandstone, southern Utah: Journal of Structural Geology, v. 161. DOI: 10.1016/j.jsg.2022.104664.

Trudgill, B., and Cartwright, J., 1994, Relay-Ramp Forms and Normal-Fault Linkages, Canyonlands National-Park, Utah. Geological Society of America Bulletin, v. 106, p. 1143 - 1157.

KECK Geology Consortium
Learning Science Through Research
Published by the Keck Geology Consortium
Short Contributions
Keck Geology Consortium
Volume 35
May 2023
doi: 10.18277/AKRSG.2023.35.03

MODELING THE SEVIER FAULT ZONE, SOUTHERN UTAH: VALIDITY TESTING AND 3D ANALYSIS

JASPER NEATH, Trinity University
Project Advisor: Benjamin Surpless

ABSTRACT

The Sevier fault zone near Orderville, Utah, represents a segmented normal fault system within the transition zone between the Basin and Range Province and the Colorado Plateau. This fault system consists of three primary segments: the Orderville segment, the Spencer Bench segment, and the Mt. Carmel Segment. The interactions between segments led to the development of complex structural geometries exposed along the fault zone. These geometries influence deformation and create fractures that affect expected permeability and fluid flow within the fault zone. These geometries also impact how slip-related energy is dissipated during earthquake-related slip propagation. Therefore, analysis of these geometries has implications for fluid flow and seismic hazard within segmented fault systems.

I used the Move2020 software suite by Petex to develop a 3D model of the complexly-segmented Sevier fault zone near the city of Orderville in southern Utah. Earlier researchers' subsurface interpretations were based on surface mapping rather than direct documentation of subsurface fault and layer geometries, so 3D model development permits validation of hypothesized subsurface structures. I digitized geologic contacts, faults, and stratigraphic horizons based on published geologic mapping and cross-sections to develop a 3D model of the fault network. I confirmed that the model does represent a well-constrained 3D system of the Sevier fault zone based on demonstrated integrity between the digital elevation model (DEM), and all available structural data. This work should provide future researchers with the data necessary to model evolution of the overall fault system, which will permit accurate determination of fault-related fracture development and the most likely fluid flow paths. Furthermore, development of a fully retro-deformable model of the fault zone will allow strain analysis that may help researchers understand how fault segment geometries impact earthquake slip propagation. This determination can be used to provide a conceptual framework for other researchers to better constrain the evolution of segmented fault zones worldwide.

INTRODUCTION

Segmented fault zones like the Sevier fault zone consist of many shorter normal faults that act as a continuous, corrugated fault (Ferrill et al. 1999). As fault segments interact, they form fractures, thus developing fluid flow pathways. Additionally, segmentation enables energy dissipation across the fault zone, which may impact seismic hazard and slip propagation across the region. By developing detailed three-dimensional structural models, we can better assess the spatial and temporal evolution of both fluid flow and slip propagation. Although fault growth through linkage and relay ramp formation is well known, the influence on three-dimensional fault geometry as a result of this process is not well understood (e.g., Fossen and Rotevatn, 2016). Three-dimensional modeling techniques allow me to perform analysis necessary to make interpretations about fault geometry that other methods cannot adequately address (Rotevatn et al. 2019).

I used the Move2020 modeling suite by Petex to develop a 3D model of the Sevier fault zone near Orderville, Utah. I used Move2020 because this program permits integration of digital elevation models (DEMs), geologic maps, orthophotography,

and cross-sections into a single model. I successfully completed four key aspects of this digitized model in Move2020: 1) I accurately aligned the geologic map of the area with the digital elevation model; 2) I precisely placed cross-sections along mapped section lines; 3) I digitized fault and horizon lines onto each section; and 4) I interpolated these lines across sections to develop 3D fault planes and stratigraphic contacts. This model will permit future workers to evaluate fracture formation, fluid flow pathways, and seismic hazard across the segmented normal fault system. This work should provide a conceptual framework for the evolution of segmented normal fault zones worldwide, especially where those fault systems are poorly exposed or in the subsurface.

STRUCTURAL BACKGROUND

The Sevier fault zone is located within the transition zone between the Basin and Range Province and the Colorado Plateau (Fig 1). The fault zone is located within the Intermountain Seismic Belt, which has had numerous historic 7.0+ magnitude earthquakes (e.g., Christenson and Nava, 1992). Additionally, the extension in this transition zone allowed for a combination of both soft and hard fault linkage across the zone. This linkage is associated with minor fault segments and the four relay ramps located within the fault zone (Fig 2). Displacement is accommodated via two capture mechanisms. The primary capture method relies on the growth and development of dominant faults within the fault system. Dominant faults, which accommodate the most displacement, propagate laterally and transfer strain between them by relay ramp development (Crider and Pollard, 1998). The other linkage mechanism relies on the overlap of two faults where one fault hard links with the other and captures the displacement of the other fault within the system (Ferrill et al. 1999).

Schiefelbein's (2002) conclusions confirm the existence of these two types of linkage mechanisms along the Sevier fault zone near Orderville. The first subtype links the fault via fault capture in the Orderville relay ramp area (Fig. 2). The second linkage subtype occurs as a result of overlapping faults with a series of cross faults and relay ramps in the Stewart Canyon overlap zone (Schiefelbein, 2002)

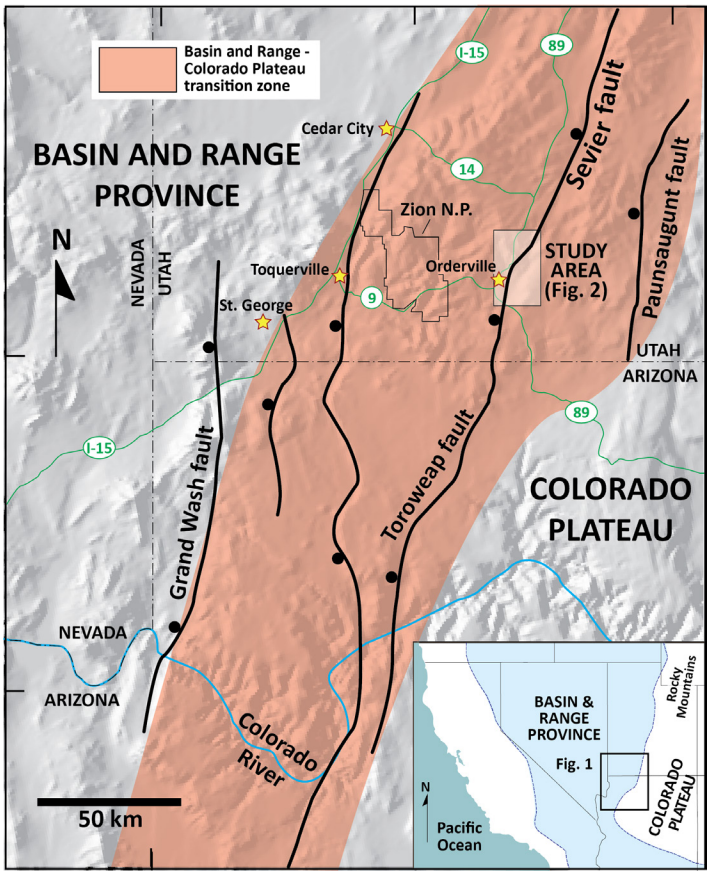

Figure 1. Transition zone between the Basin and Range Province and the Colorado Plateau displaying the primary faults that accommodate extension (modified from Thelin and Pike, 1991; Reber et al., 2001).

(Fig. 2).

Two models of fault growth, the propagating fault model and the constant length fault model, provide frameworks to help explain the growth of normal fault segments. The propagating fault model asserts that fault growth occurs primarily due to the lengthening and linkage of individual, initially independent fault segments (e.g., Rotevatn et al. 2019). Meanwhile, the constant length fault model explains that rather than growing through a lengthening and linkage process over time, faults instead propagate to their near-full lengths rapidly. This propagation is typically associated with mechanical interactions between adjacent fault segments and a reduction in tip stresses (Rotevatn et al. 2019). The digitized 3D model of the Sevier fault zone that I have constructed can be used to test these end-member models. In addition to the variety of capture methods associated with different linkage types, damage zones, commonly highly-fractured rock, form as a result of fault displacement and interaction. These damage zones

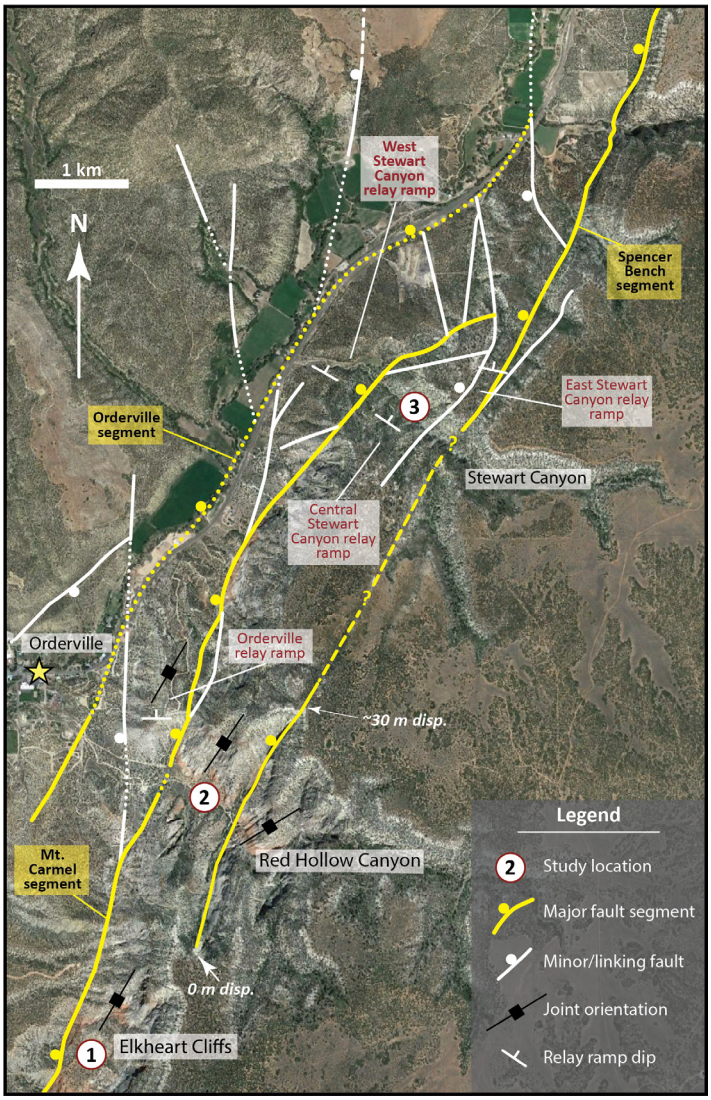

Figure 2. Structural map of the fault network within the Sevier fault zone at Orderville. Thick yellow lines are primary segments of the Sevier fault zone (Simoneau et al., 2016; Hankla et al., 2019).

are classified based on the structural position of the damage. Damage zones form along the tip, wall, or linkage zone between fault segments (e.g., Long and Imber, 2011). These damage zones are commonly associated with the breaching of relay ramps between dominant segments of the Sevier fault zone. These damage zones release stresses associated with fault tip propagation and may serve as conduits for fluid flow (e.g., Fossen and Rotevatn, 2016).

METHODS

I designed an eight-step modeling workflow in order to efficiently develop a high-resolution model of the Sevier fault zone (Fig 3). I performed all steps of the modeling workflow except for the Georeference Geologic Map step, which I completed in ARC-GIS,

Georeference Geologic Map	• Use ArcGIS to georeference geologic map of the study area.
Import Required Data	• Import required digital elevation model (DEM), cross-sections, orthophotos, and drape the georeferenced geologic map over the DEM.
Trace Sections Over Map	• Trace lines of section across the map to work in section view and link each cross-section within its associated section line.
Transform Cross-Sectional Interpretations	• Transform each cross-section to best fit the topography/DEM profile.
Trace Structural and Stratigraphic Features	• Trace synclines, anticlines, faults, and other structures in map view. • Digitize all faults and straigraphic horizons in cross-sectional view.
Create Surfaces	• In 3D view, interpolate both digitized faults and horizons between lines of section to create 3D surfaces that can be used for visualization and later analysis.
Validate and Restore Model	• Calculate the horizon lengths in the *2D Section Analysis* module. If the lengths don't balance, use the *2D and 3D Move on Fault* modules to revise cross-sections for consistency.
Restoration and Forward Modeling	• Reconstruct line horizons and surfaces from the restored sections. Forward modeling and Monte Carlo simulations can be performed to test models of fault network evolution.

Figure 3. Eight-step modeling workflow used to develop a high resolution model of the Sevier fault zone.

within Move2020. The restoration and reconstruction steps only need to be completed if 2D section analysis reveals the horizon lengths to be inconsistent. An example of a model created prior to restoration with this modeling workflow is shown below (Fig. 4). I completed through step 6 of the modeling workflow, the Create Surfaces step. Completion of this step relies on interpolating fault and line horizons across multiple cross-sections in order to translate 2D data into 3D space. The primary data I used for this process, imported during the Import Required Data step, were cross-sections and a geologic map created by Schiefelbein (2002). The majority of these cross-sections were constructed in the southern portion of the geologic map, where there is sufficient data density, so I focused on the southern portion of the map area to assess the most complex portion of the fault system.

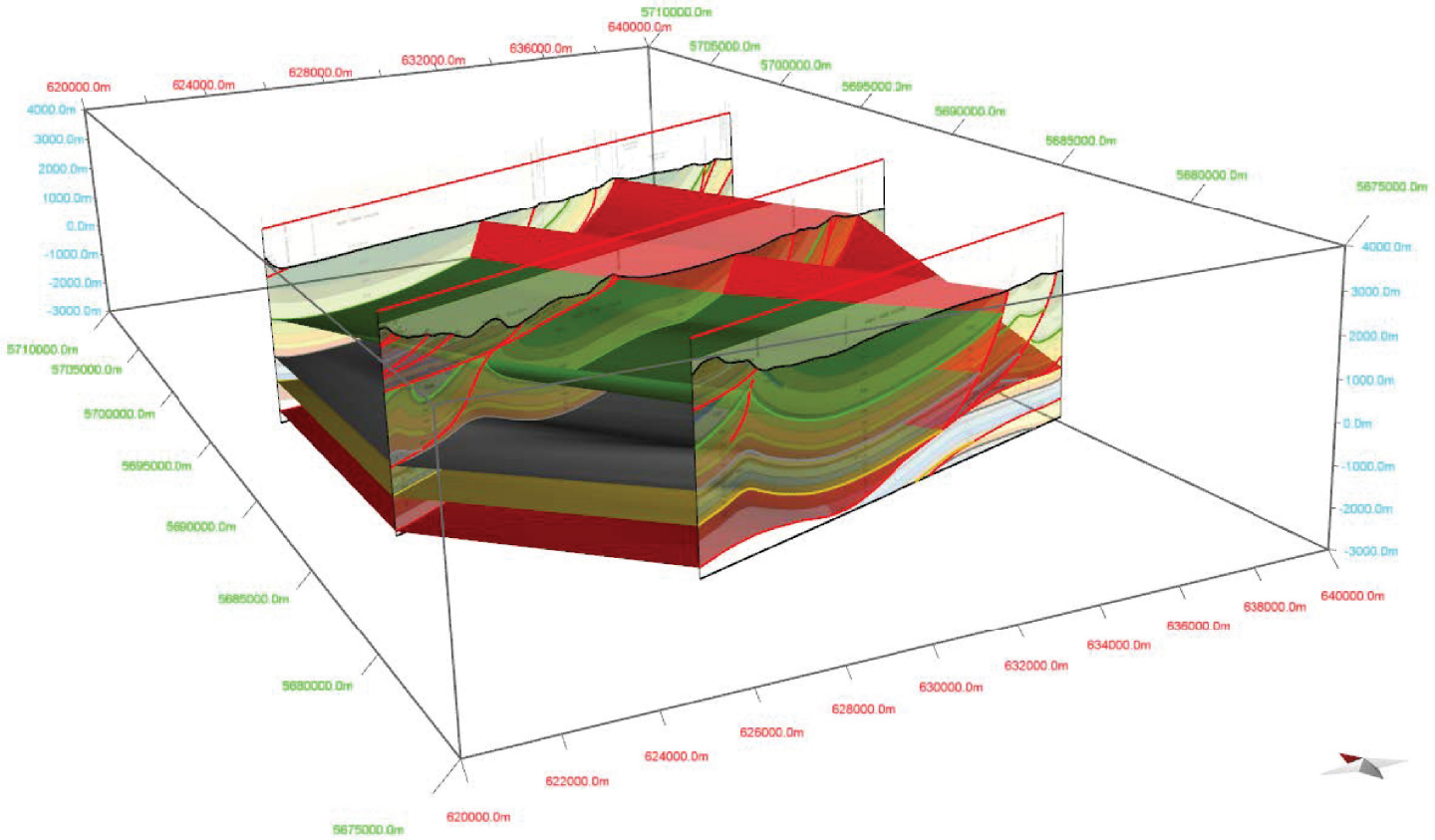

Figure 4. Completed 3D model prior to validation and restoration. This example was created using the modeling workflow shown in Figure 3.

RESULTS

I succeeded in developing a well-constrained 3D model of the Sevier fault network near Orderville, Utah. My model demonstrates integrity between the DEM, geologic map, cross-sections, and stratigraphic horizon displacements. I have been able to evaluate displacement gradients across the fault zone by aligning the georeferenced geologic map, DEM, and cross-sections within section lines. Additionally, I successfully demonstrated the general validity of the original cross-sectional interpretations by establishing line-length consistency across and between cross-sections. I have used my model to document along-strike changes in displacement of a stratigraphic horizon surface along a fault plane where subsurface interpretations have been validated (Fig 5). However, my analysis revealed that some of Schiefelbein's (2002) initial interpretations need to be slightly revised. For instance, I found certain upper horizon lengths to be shorter than lower horizon lengths in Schiefelbein's (2002) cross-sectional interpretations. Once these structural interpretations have been validated across the fault network, future researchers will able to assess fault geometries along the fault zone and limit possible kinematic fault evolution scenarios.

FUTURE WORK

Future work must address the discrepancy in data density between the northern and southern sections of the study area. Specifically, future researchers will need to use surface data to construct more cross-sections in the northern Sevier fault study area. These cross-sections will need to undergo the same validation process that I performed on Schiefelbein's (2002) cross-sections. Additionally, future researchers will need to revise some of Schiefelbein's (2002) structural interpretations. To address discrepancies, researchers may add blind faults at depth, adjust changes in displacement magnitudes/ratios with depth, and/or change fault geometries. This work will allow us to answer the following research questions: 1) Are modeling results consistent with the established ideas about the kinematics of segmented fault zone evolution? 2) How do permeability and fluid flow

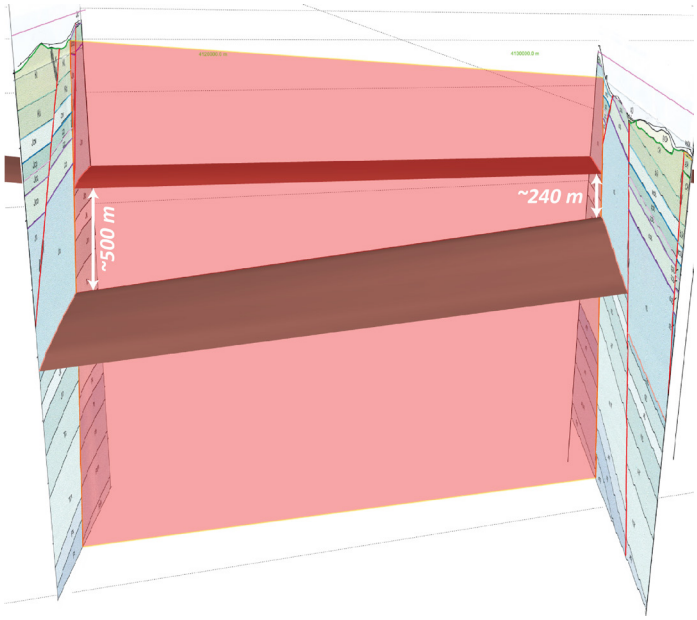

Figure 5. Displacement of a layered horizon (shown in brown in foreground and dark red in background) by a fault surface (shown in transparent light red) along the Sevier fault zone.

pathways change as a segmented fault zone evolves? and 3) How can these results be used to assess the impacts of fault geometry on the propagation of slip during an earthquake?

IMPLICATIONS

The structural geometries and features exposed along the Sevier fault zone are important because they influence deformation within the rock volume, creating fractures that affect permeability and fluid flow within the fault zone. Therefore, the geometry of the system in the subsurface affects groundwater flow. By validating and revising previous interpretations of the Sevier fault zone, researchers will be able to accurately determine the evolution of the fault system and related fluid flow paths. This structural evolution will provide a conceptual framework that other researchers can use to better constrain the evolution of segmented fault zones worldwide.

Furthermore, analysis of the structural geometries and features exposed along the Sevier fault zone may allow for analysis of fault damage zones, best characterized by fracturing. These damage zones absorb some portion of energy related to earthquake slip propagation (e.g., Surpless and McKeighan, 2022). Additionally, segmented portions of major faults impede the propagation of slip due to their complex geometries. If a fully retro-deformable model of the fault zone can be completed, this model would allow for fracture and strain analysis associated with the creation of damage zones. In turn, this model might help researchers better understand how damage zones evolve over time in segmented fault zones, and more specifically might aid in understanding how fault segment geometries impact earthquake slip propagation.

ACKNOWLEDGMENTS

This material is based upon work supported by the Keck Geology Consortium and the National Science Foundation under Grant No. 2050697. It was also supported by NSF Award 2042114 to PI Surpless. Finally, funding was provided by the Geosciences Department at Trinity University, including funding from the Roy and Tinker Funds to support undergraduate student research.

REFERENCES

Christenson, G.E. and Nava, S.J., 1992, Earthquake Hazards of southwestern Utah, In Harty, K.M., ed., Engineering and Environmental Geology of Southwestern Utah: Utah Geological Association Publication 21, p. 123-138.

Crider, J., and Pollard, D., 1998, Fault linkage: Three-dimensional mechanical interaction between echelon normal faults: Journal of Geophysical Research, v. 103, p. 24,373 – 24,391.

Hankla, C., and Judge, S., 2019, An analysis of fractures around the Sevier fault zone in Red Hollow Canyon near Orderville, Utah: Keck Geology Consortium, Volume of Short Contributions, v. 32, 7 p.

Ferrill, D.A., Stamatakos, J.A., and Sims, D., 1999, Normal fault corrugation: implications for growth and seismicity of active normal faults: Journal of Structural Geology, v. 21, p. 1027-1038.

Fossen, Haakon, and Rotevatn, Atle, 2016, Fault linkage and relay structures in extensional settings–A review: Earth Science Reviews, v. 154, p. 14-28.

Long, J., and Imber, J., 2011, Geological controls on fault relay zone scaling: Journal of Structural Geology, v. 33, p. 1790 – 1800.

Reber, S., Taylor, W., Stewart, M., and Schiefelbein, I., 2001, Linkage and Reactivation along the northern Hurricane and Sevier faults, southwestern Utah, In M.C. Erskine, J.E. Faulds, J.M. Bartley, and P.D. Rowley, Eds., The Geologic Transition, High Plateaus to Great Basin – A Symposium and Field Guide, The Mackin Volume: Utah Geological Association Publication 30, Pacific Section American Association of Petroleum Geologists Publication GB78, p. 379 – 400.

Rotevatn, A., Jackson, C.A-L., Tvedt, A.B.M, Bell, R.E., Blaekkan, I., 2019, How do normal faults grow?: Journal of Structural Geology, v. 125, p. 174-184.

Schiefelbein, I., 2002, Fault segmentation, fault linkage, and hazards along the Sevier fault, southwestern Utah [M.S. thesis]: Las Vegas, University of Nevada at Las Vegas, 132 p.

Simoneau, S., Surpless, B., and Mathy, H., 2016, The evolution of subsidiary fracture networks in segmented normal fault systems: GSA National Meeting, Abstracts with Programs, Denver, Colorado.

Surpless, B., and McKeighan, C., 2022, The role of fracture branching in the evolution of fracture networks: An outcrop study of the Jurassic Navajo Sandstone, southern Utah: Journal of Structural Geology, v. 161, 17 p.

Thelin, G.P., and Pike, R.J., 1991, Landforms of the Conterminous United States - A Digital Shaded-Relief Portrayal: U.S.G.S. Geologic Investigations Series I – 2720.

KECK Geology Consortium
Learning Science Through Research
Published by the Keck Geology Consortium
Short Contributions
Keck Geology Consortium
Volume 35
May 2023
doi: 10.18277/AKRSG.2023.35.04

NORMAL FAULT-TIP DAMAGE ZONE STRUCTURES AND GEOMETRIES FROM THE SEVIER FAULT, UTAH

MICHELLE NISHIMOTO, Wellesley College
Project Advisor: Katrin Monecke

INTRODUCTION

Fractures within rocks form due to differential stresses that exceed rock strength. The magnitude and orientation of the local stress field depends on tectonic setting and influences the extent and direction of fracture initiation and propagation. Understanding fracture network characteristics and geometries is fundamental to answer various geological research questions. Studies by Ampuero and Mao (2017) and others have shown the importance of understanding the geometry and intensity of fracturing at and adjacent to faults when evaluating earthquake hazards. In addition, fracturing and the resultant porosity and permeability of a rock affect fluid flow and the potential for geothermal energy transfer (e.g., Siler et al., 2018). Furthermore, fracture pattern analysis may reveal potential asymmetry of fracture intensity across a fault (e.g., Berg and Skar, 2005) and how normal faults grow over time (e.g., Nicol et al., 2016).

For this study, I analyzed the fracture pattern of the isolated normal fault tip zone of the Spencer Bench segment from the Sevier fault using traditional geological field methods as well as a relatively new approach based on analysis of virtual outcrop models built from drone imagery. Both field measurements and virtual outcrop data are used to map the scale and type of fracturing in the fault core and across the adjacent footwall and hanging wall of the fault segment. I explore how fracture intensity varies within the rock volume adjacent to the tip of a normal fault, the difference in fracture network characteristics between the hanging wall and footwall, and the relationship between fracture patterns and lithology.

BACKGROUND

Fault Propagation and Fault Damage Zones

Differences in bed contacts, thickness of beds, and material properties influence the formation and propagation of fractures in sedimentary rocks (e.g., Cooke et al., 2000). Fractures, including faults, initiate and propagate when stress surrounding the rock exceeds rock strength. The extent of the fracture depends on the magnitude and orientation of the local stress field. When normal faults propagate laterally and accommodate displacement across the fault, they often produce a highly deformed fault core and a broader volume of rock deformation known as a damage zone. Based on their location along the fault, damage zones are classified as tip-, wall-, or linking-damage zones (see Fig. 3 in Surpless, this volume). Fault-tip and wall damage zones develop in response to fault propagation and displacement, caused by the local amplification of stresses parallel to the fault plane and in the fault tip regions (e.g., Kim et al., 2004). Damage zones of normal faults can further be divided into inner and outer damage zones developing adjacent to the fault (Fig. 1). As the distance from the fault core increases, the intensity of fracturing decreases to an undamaged rock volume.

Fault Damage Zone Asymmetry

Across a fault, deformation or strain is often distributed asymmetrically, resulting in differences in damage zone characteristics in the hanging wall relative to the footwall (Fig. 1). Along normal faults, the hanging-wall damage zone tends to be wider than the footwall damage zone (Liao et al., 2020). In a study looking at the spatial arrangement of fractures

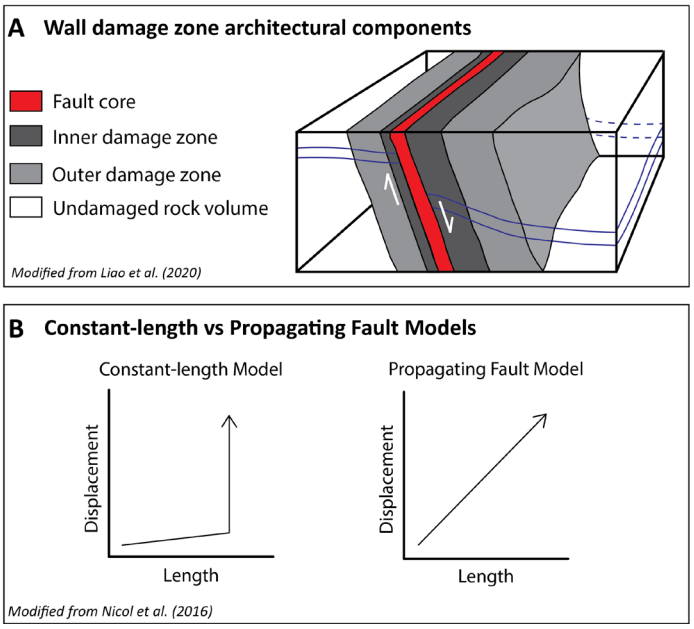

Figure 1. A) Conceptual model for an asymmetrical normal fault wall damage zone and its architectural components. Red indicates the fault core, dark gray is for the inner damage zone, gray is for the outer damage zone, and white marks the undamaged rock. The white arrows and blue lines indicate displacement along the fault and displaced hypothetical rock units. B) Evolution of displacement and length according to the constant-length model (left) and propagating fault model (right). Figure A modified from Liao et al., (2020). Figure B adapted from Nicol et al., (2016).

in the damage zone at a segment of the Moab fault in southeastern Utah, Berg and Skar (2005) found that the hanging-wall damage zone was more than three times wider than the footwall damage zone and suggest that the stress pattern that occurs during fault propagation causes an asymmetric distribution of strain.

Constant-length vs Propagating Fault Models

There are two schools of thought on how a normal fault's displacement (D) and map-view trace length (L) grow over time (Fig. 1): the propagating fault model, also known as the increasing length model or isolated fault model, and the constant-length model, also known as the coherent fault model (Fig. 1) (e.g., Cartwright et al., 1995). The propagating fault model suggests that a fault's D/L ratio stays relatively constant over successive fault movements whereas the constant-length model suggests that there is an initial phase of rapid fault propagation along strike followed by a more prolonged period of displacement accumulation on faults with near-constant lengths (Nicol et al., 2016).

Earlier studies, focused upon map-view geologic data, supported the propagating fault model (e.g., Cartwright et al., 1995). However, more recent studies based on seismic survey data (Walsh et al., 2003), comparisons of the thickness versus displacement of fault geometric components (fault rock, fault zone, breached relay zone, and intact relay zone) of a normal fault (Childs et al., 2009), and a study on a system of faults at outcrop-scale (Nicol et al., 2016) better support the constant-length model. In their study of a fault zone in central Texas, Ferrill et al. (2011) argue that a constant-length model is more consistent with their data and suggest that both fault length and damage zone width are established early and likely remain relatively constant as displacement accumulates.

Sevier Fault Zone

Along the Hurricane and Paunsaugunt normal faults, the Sevier-Toroweap normal fault accommodates strain across the transition zone between the Colorado Plateau to the East and the Basin and Range province to the West (e.g., Davis, 1999; Schiefelbein, 2002; Surpless and McKeighan, 2022) (see Fig. 1 in Surpless, this volume). The Sevier fault is a segmented fault that extends ~350 km through Utah and Arizona with a strike of ~N30°E and steep 70-85°W dip (Davis, 1999; Schiefelbein, 2002). In this study, I focus on an isolated normal fault tip near the southern end of a complexly faulted zone of the Sevier normal fault that is well exposed at the Elkheart Cliffs and the southern end of the Red Hollow Canyon by Orderville, Utah (Fig. 2 in Surpless, this volume).

METHODS

Field Methods

We conducted fieldwork near Orderville, Utah, where there is good exposure of the Spencer Bench Fault segment. At locations of interest, we collected scanline data to document the primary orientation and intensity of fracturing, with the position measured perpendicular to the dominant fracture strike. We used a Geo Transit Brunton to measure the azimuth and dip of each fracture along the scanline and constructed stereonets using Stereonet 11 by Allmendinger (2022).

Capturing Imagery with Unmanned-Aerial-Vehicle (UAV) Flights

In locations inaccessible by foot, we planned and executed a series of unmanned-aerial-vehicle (UAV) flights using a Phantom 4 Professional UAV. The 4K camera attached to the drone recorded video imagery of canyon walls and cliff faces across the fault network. We documented the spatial extent of each drone flight on Google Earth Professional and described the content of each video in a field book.

Building virtual outcrop models (VOMs) using Structure-from-Motion (SfM) software

We used videos taken by the UAV flights to build virtual outcrop models (VOMs) using Agisoft Metashape, structure-from-motion (SfM) software designed to build 3D outcrop models based on overlapping aerial images (Metashape, 2023) (Fig. 2). We created 2D orthomosaics from the georeferenced VOMs, which we annotated in Metashape. Where best exposed, we documented displacement across the fault core. We set up virtual scanlines drawn perpendicular to fractures, measuring the position of fractures along each scanline and conducted statistical analysis on the collected scanline data. Values derived include the average spacing between fractures (m), the fracture spacing standard deviation (m), position-based fracture intensity (FI) (m^{-1}), scanline average FI (m^{-1}), and coefficient of variation (CV =σ/μ).

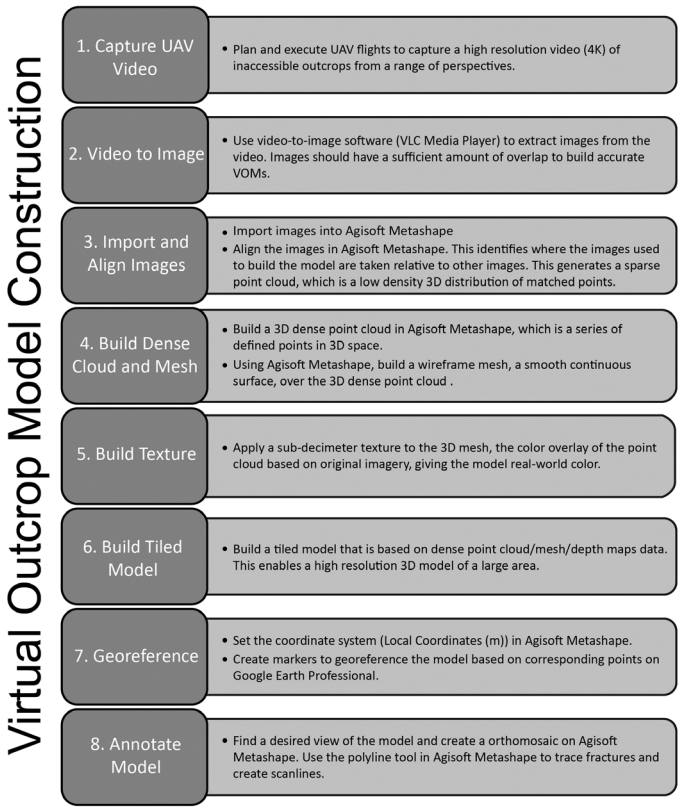

Figure 2. Steps for VOM model construction and analysis. Workflow to construct a spatially accurate 3D outcrop model using Agisoft Metashape. Figure modified from Surpless and McKeighan, 2022.

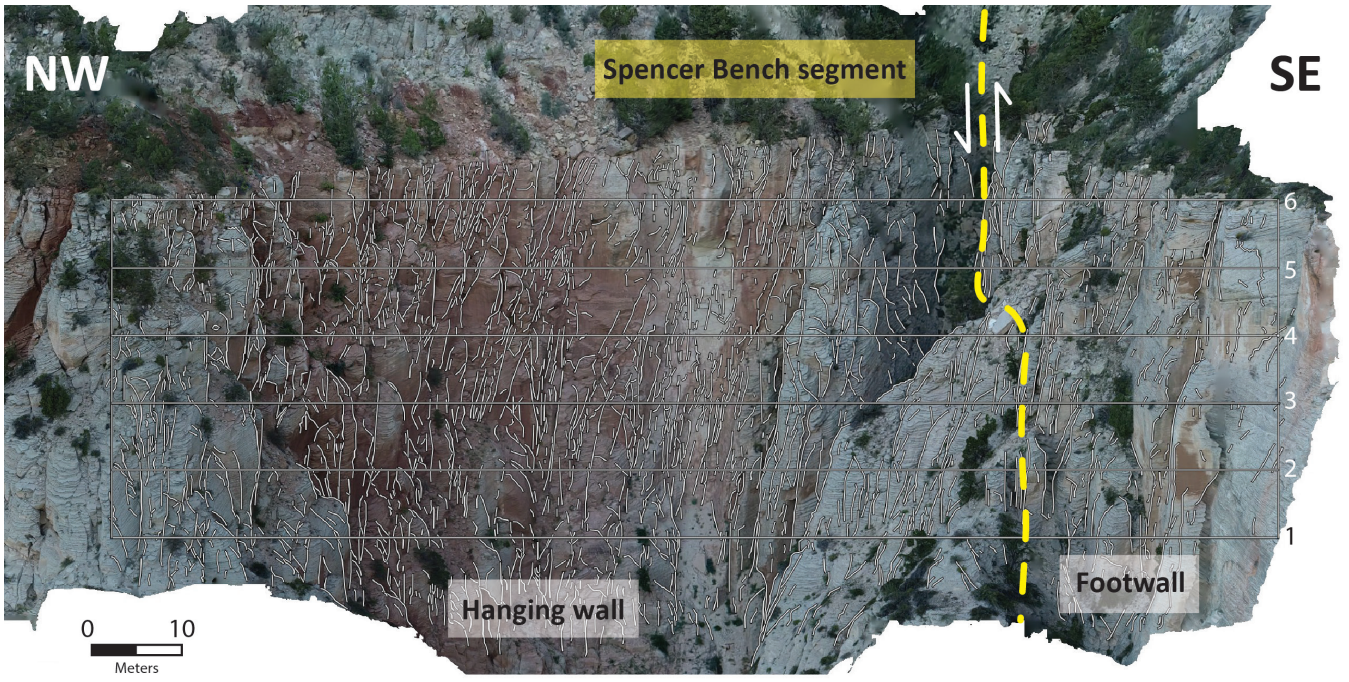

Figure 3. Orthomosaic of Model 3 where the Spencer Bench segment can be seen passing through the model. Yellow dashed lines show the suggested locations where the Spencer Bench segment passes through. White lines trace the fractures observed. White horizontal lines indicate the location of the scanlines.

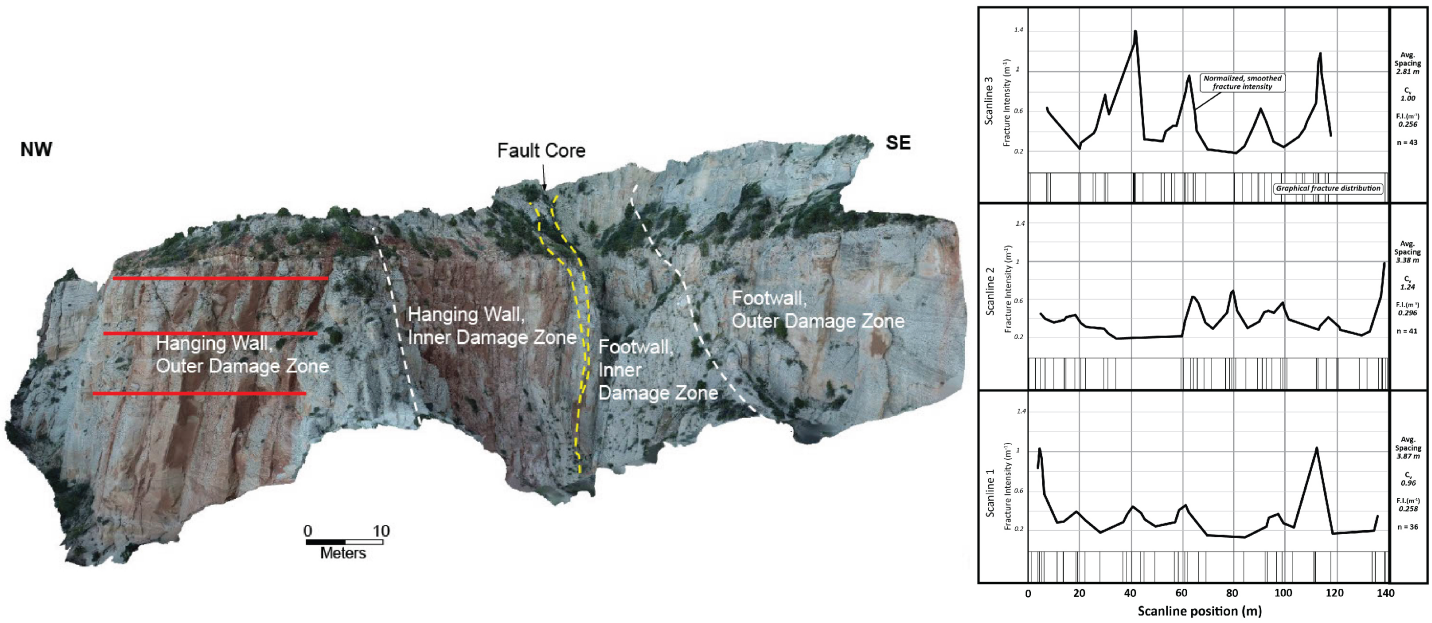

Figure 4. Fault damage zone asymmetry of Model 3 and FI along scanlines. Model 3 shows the Navajo Sandstone across the Spencer Bench segment (yellow). Red lines indicate where scanline data were collected.

RESULTS

Field-Based Scanline Analysis

We collected scanline data at 11 locations within the fault zone of the Mt. Carmel and Spencer Bench segments, focusing on the well-exposed Navajo Sandstone. We measured fractures greater than 4 meters along field scanlines that intersected the strike of the fractures. Overall, most fractures strike NE to NNE and dip moderately to steeply NW, subparallel to the fault segments. The average FI ranged between 0.19 m^{-1} and 6.31 m^{-1}.

Fault Damage Zone Asymmetry

Observations from Model 3, at Elkheart Cliffs with the Spencer Bench segment located on the SE side of the model, support the analysis performed by Liao et al., (2020) and Berg and Skar (2005), who suggested that wall damage zones display greater widths of both inner and outer damage in the hanging wall relative to the footwall (Figs. 3 and 4). This asymmetry may result from preferential fracture rupture propagation caused by footwall-hanging wall differences in local stress fields around normal fault planes (e.g., Ampuero and Mao, 2017). Our finding is significant given we documented damage zone widths based on outcrop exposures, unlike Liao et al., (2020), where seismic data were used to identify the asymmetry.

Constant-length vs Propagating Fault Models

A comparison of the widths of the footwall damage zone of the Mt. Carmel and Spencer Bench segments at the same latitude shows near-identical dimensions (Fig. 5). However, the displacement across the Mt. Carmel segment is approximately 800 meters (McKeighan et al., 2019), while the displacement across the Spencer Bench segment is only about 2 meters. This suggests that the two faults at this latitude are at different stages of fault propagation and that

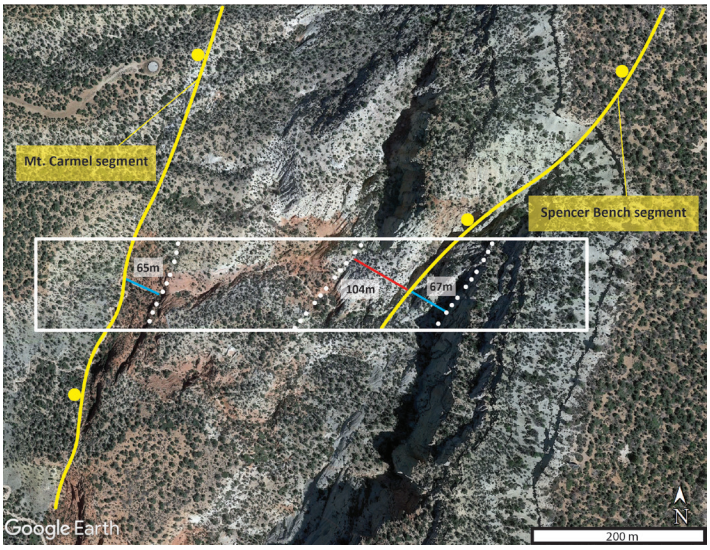

Figure 5. Comparison of the width of the footwall damage zones of the Mt. Carmel and Spencer Bench segments (blue) at the same latitude. Width measurements are taken perpendicular to the fracture orientation from Google Earth Professional.

the footwall damage zone width is established very early in fault propagation. New damage will likely be localized in the already established damage zone (e.g., Ferrill et al., 2011). In addition, McKeighan et al. (2019) identified displacement of 30 meters across the Spencer Bench segment approximately 2.5 kilometers North of where we measured a displacement of only 2 meters in Model 2. This yields a low lateral displacement gradient of 0.0112. Together, this suggests relatively rapid lateral propagation of the Spencer Bench segment with little accumulated displacement. These data strongly support the constant-length model.

ACKNOWLEDGMENTS

This material is based upon work supported by the Keck Geology Consortium and the National Science Foundation under Grant No. 2050697. It was also supported by NSF Award 2042114 to PI Surpless. I would like to extend my deepest gratitude to Dr. Benjamin Surpless and Dr. Katrin Monecke for their continuous support throughout this project.

REFERENCES

Allmendinger, R., 2022. Stereonet 11: accessed January, 2023, https://www.rickallmendinger.net/stereonet/

Ampuero, J. P., and X. Mao, 2017, Upper limit on damage zone thickness controlled by seismogenic depth, in M. Y. Thomas, T. M. Mitchell, and H. S. Bhat, eds., Fault zone dynamic processes: Evolution of fault properties during seismic rupture: American Geophysical Union, doi: 10.1002/9781119156895.ch13.

Berg, S., and T. Skar, 2005, Controls on damage zone asymmetry of a normal fault zone: Outcrop analyses of a segment of the Moab fault, SE Utah: Journal of Structural Geology, 27, 1803–1822, doi: 10.1016/j.jsg.2005.04.012.

Cartwright, J.A., Trudgill, B.D., and Mansfield, C.S., 1995, Fault growth by segment linkage: an explanation for scatter in maximum displacement and trace length data from the Canyonlands Grabens of SE Utah: Journal of Structural Geology, v. 17, no. 9, p. 1319-1326.

Childs, C., Manzocchi, T., Walsh, J.J., Bonson, C.G., Nicol, A., and Schopfer, M.P.J., 2009: A geometric model of fault zone and fault rock thickness variations: Journal of Structural Geology, v. 31, p. 117-127.

Cooke, M., Mollema, P., Pollard, D., and Aydin, A., 2000, Interlayer slip and joint localization in the East Kaibab Monocline, Utah: field evidence and result from numerical modeling, In Cosgrove, J., and Ameen, M., eds.: Forced Folds and Fractures, Geological Society, London, v. 169, p. 23-49.

Davis, G., 1999, Structural geology of the Colorado Plateau region of southern Utah, with special emphasis on deformation bands: Geological Society of America Special Paper 342, p. 157.

Ferrill, D.A., Morris, A.P., McGinnis, R.N., Smart, K.J., and Ward, W.C., 2011, Fault zone deformation and displacement partitioning in mechanically layered carbonates: the Hidden Valley fault, central Texas: The American Association of Petroleum Geologists, v. 95, no. 8, p. 1383-1397.

Kim, K.S., Peacock, D., and Sanderson, D., 2004, Fault damage zones: Journal of Structural Geology, v. 26, p. 503– 517.

Liao, Z., Hu, L., Huang, X., Carpenter, B., Marfurt, K., Vasileva, S., Zhou, Y., 2022, Characterizing damage zones of normal faults using seismic variance in the Wangxuzhuang oilfield, China: Interpretation, v. 8, doi: 10.1190/INT-2020-0004.1.

Metashape, Agisoft, 2023. Agisoft Metashape User Manual (pdf): accessed March, 2023.https://www.agisoft.com/pdf/metashape-pro_2_0_en.pdf. version 2.0.

McKeighan, C., and Surpless, B., 2019, Analyzing Deformation within a Normal Fault Transfer Zone Using SfM 3D Modeling: Keck Geology Consortium, Volume of Short Contributions, v. 32, 7 p.

Nicol, A., Childs, C., Walsh, Manzocchi, T., and Schopfer, M.P.J., J.J., 2016, Interactions and growth of faults in an outcrop-scale system: Geological Society of London, v. 439, p. 23-39, doi: 10.1144/SP439.9

Schiefelbein, I.M., 2002, Fault segmentation, fault linkage, and hazards along the Sevier fault,southwestern Utah [M.S. thesis]: Las Vegas, University of Nevada at Las Vegas, 132 p.

Siler, D.L., Hinz, N.H., Faulds, J.E., Tobin, B., Blake, K., Tiedeman, A., Sabin, A., Lazaro, M., Blankenship, D., Kennedy, M., Rhodes, G., Akerley, J., Hickman, S., Glen, J., Williams, C., Robertson-Tait, A., Pettitt, W., 2018, An Update on the Geologic Model of the Fallon FORGE site. Geothermal Research Council Transactions, v. 41, p. 11-21.

Surpless, B., 2023, Structural Evolution of the segmented Sevier fault, southern Utah: Keck Geology Consortium, Volume of Short Contributions, v. 36, 7 p.

Surpless, B., and McKeighan, C., 2022, The role of dynamic fracture branching in the evolution of fracture networks: an outcrop study of the Jurassic Navajo Sandstone, southern Utah: Journal of Structural Geology, v. 161. doi: 10.1016/j.jsg.2022.104664.

Walsh, J.J., Bailey, W.R., Childs, C., Nicol, A., and Bonson, C.G., 2003: Formation of segmented normal faults: a 3-D perspective: Journal of Structural Geology, v. 25, p. 1251-1262.